ACS OMEGA

http://pubs.acs.org/journal/acsodf

Article

Carbazole/Benzimidazole-Based Bipolar Molecules as the Hosts for Phosphorescent and Thermally Activated Delayed Fluorescence Emitters for Efficient OLEDs

Zhen-Jie Gao, Tzu-Hung Yeh, Jing-Jie Xu, Chih-Chien Lee, Anuradha Chowdhury, Bo-Cheng Wang,* Shun-Wei Liu,* and Chih-Hsin Chen*

Cite This: *ACS Omega* 2020, 5, 10553−10561

Read Online

ACCESS | Metrics & More | Article Recommendations | Supporting Information

ABSTRACT: A series of carbazole/benzimidazole-based molecules, namely, *o*-CbzBiz, *m*-CbzBiz, and *p*-CbzBiz, were readily synthesized in three steps by integrating carbazole with benzimidazole via the *ortho*-, *meta*-, and *para*-positions of phenyl linked to *N*-phenyl carbazole. These bipolar molecules exhibited a maximum UV absorption band ranging from 310 to 327 nm and a maximum emission band ranging from 380 to 400 nm. Density functional theory calculations showed that the twist angles between the donor and acceptor moieties of these molecules were from 54.9 to 67.1°. Such a twisted structure hampered the π-electron conjugation within the molecule and resulted in high-lying LUMO levels and triplet energies, which make them suitable to be applied as host materials in OLED devices. Our results showed that a maximum external quantum efficiency (EQE) of OLED reached 21.8% when *p*-CbzBiz was applied as the host of a green phosphorescent emitter, i.e., $Ir(ppy)_2(acac)$. In addition, a maximum EQE of OLED reached 16.7% when *o*-CbzBiz with the host of a green TADF emitter, i.e., 4CzIPN. Moreover, these devices exhibited lower efficiency roll-off than the CBP-hosted device using the same emitters, which demonstrated the bipolar charge carrier property of carbazole/benzimidazole-based molecules.

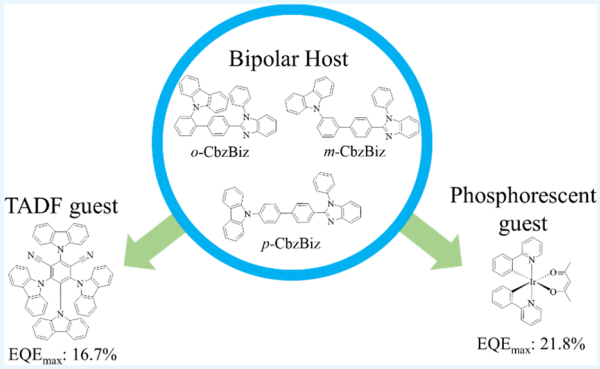

INTRODUCTION

In recent years, organic light-emitting diodes (OLEDs) have become a popular technique for display-related products such as smartphones and televisions because they are thinner, lighter, and more flexible than conventional LCD displays.[1−4] For high device performance of OLEDs, researchers have endeavored to develop the organic materials with ideal photophysical and electrochemical properties. Specifically, phosphorescent and thermally activated delayed fluorescence (TADF) emitters have been considered as the most promising emitters for OLEDs because they can harvest both singlet and triplet excitons through intersystem crossing and reverse intersystem crossing, which allows the internal quantum efficiency of OLEDs to potentially achieve 100%.[5−8] Because triplet excitons are prone to quench at high concentration through triplet−triplet annihilation, phosphorescent and TADF-based OLEDs usually apply a host−guest systems to optimize the performance of the device. An ideal host−guest system relies on the subtle balance of charge carrier transporting between the host and the guest molecules. Therefore, the development of host materials that could pair with highly efficient emitters in the host−guest system is critically needed.[9−12]

In past studies, carbazole-based molecules, e.g., 4,4′-bis(9-carbazolyl)-2,2′-biphenyl (CBP) and 1,3-bis(9-carbazolyl)-benzene (mCP), are often used as the host materials for OLEDs with high external quantum efficiency (EQE) due to their high triplet energy levels. However, both molecular structures of CBP and mCP are constructed by benzene and an electron-donating moiety, i.e., carbazole, such that they are classified as unipolar molecules. This feature would lead to unbalanced charge-transporting in the emitting layer (EML) when CBP and mCP are applied as the host of OLEDs.[13−15] As a result, the charge recombination zone of such devices is closer to the interface between EML and electron-transporting layer (ETL) or hole-transporting layer (HTL), leading to a narrower recombination zone and inferior performance at higher applied voltage and brightness of the device.[16,17] Compared with unipolar molecules, bipolar molecules have

Received: March 4, 2020
Accepted: April 3, 2020
Published: May 3, 2020

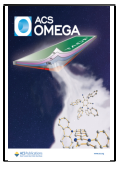

Scheme 1. Synthetic Routes and Molecular Structures for *o*-CbzBiz, *m*-CbzBiz, and *p*-CbzBiz

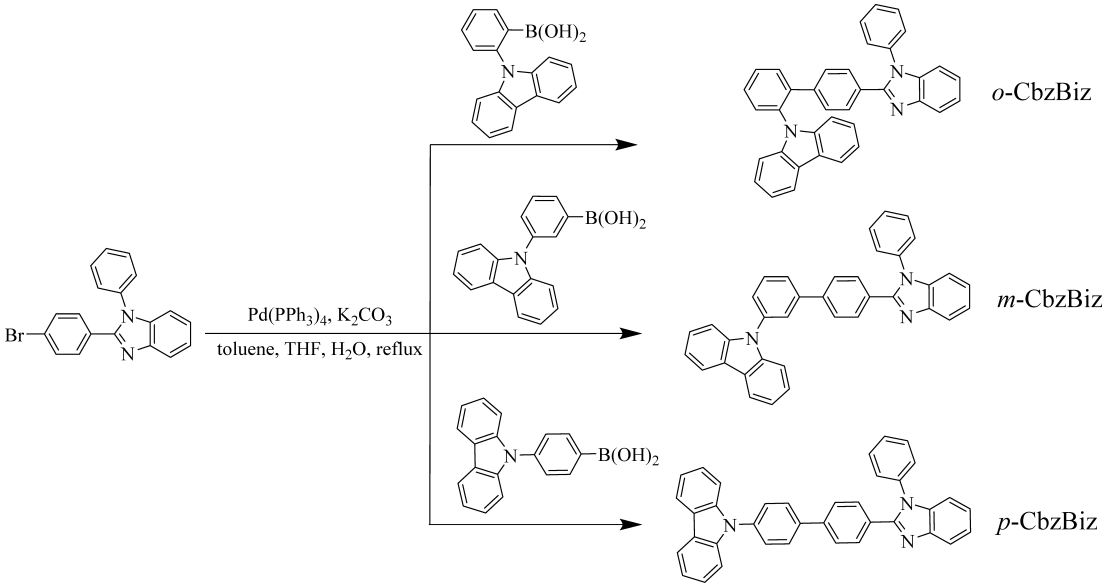

also been applied as the host materials for OLEDs due to their balanced hole- and electron-transporting capability that could be beneficial to improve the device performance.[18−20] For example, Wang et al. reported that, when electron-withdrawing moieties such as pyridine, benzimidazole, and triazine were introduced to the molecular structure of CBP as the host materials of phosphorescent OLEDs using $Ir(ppy)_3$ as the emitter, the EQEs of the devices were 17.1−18.9%, which were significantly higher than that of the CBP-based device (EQE = 13.8%).[21] On the other hand, Song et al. reported that electron-withdrawing [1,2,4]triazolo[1,5-*a*]pyridine can be integrated with carbazole to construct the host materials for phosphorescent and TADF OLEDs with high EQE.[22] These results demonstrated that carbazole-based bipolar molecules are potential ideal host materials for OLED applications.

Benzimidazole-based molecules, e.g., 2,2,2-(1,3,5-phenylene)-tris(1-phenyl-1*H*-benzimidazole) (TBPi), are well-known electron-transporting materials in OLED applications due to their high electron mobility. In past studies, benzimidazole has also been used to construct bipolar molecules that can serve as hole-transporting materials, emitters, and hosts for fluorescence or phosphorescence OLEDs with high performances.[2,23] However, research on benzimidazole-based molecules as the host materials for TADF OLEDs is still rare. To date, Zhao et al. published the only paper about benzimidazole-based molecules as the host materials for TADF OLEDs. In their study, the EQE reached 18.7% for the OLED that applied 9,9′-(2′-(1*H*-benzimidazol-1-yl)-[1,1′-biphenyl]-3,5-diyl)bis(9*H*-carbazole) (*o*-mCPBI) as the host and 4CzIPN as the green TADF emitter, demonstrating the feasibility of benzimidazole-based molecules as the host materials for TADF OLEDs.[24]

In this work, we synthesized three carbazole/benzimidazole-based bipolar molecules, namely, *o*-CbzBiz, *m*-CbzBiz, and *p*-CbzBiz. In these molecules, carbazole was integrated with the benzimidazole moiety via the *ortho*-, *meta*-, and *para*-positions of phenyl linked to *N*-phenyl carbazole. All these molecules were readily obtained through three synthetic steps. Their thermal stability, photophysical, and electrochemical properties as well as the performance of OLED by using *o*-CbzBiz, *m*-CbzBiz, and *p*-CbzBiz as host materials were characterized. Because the energy level of triplet excited states was affected by the spatial overlap between the highest occupied molecular orbital (HOMO) and lowest unoccupied molecular orbital (LUMO) for a bipolar molecule, it has been demonstrated that the triplet energy of host materials can be tuned through adjusting the twist angle between the donor and acceptor moieties of a bipolar molecule.[25,26] Therefore, we investigated how molecular geometries of the host materials affect their photophysical and electrochemical properties and corresponding device performance.

RESULTS AND DISCUSSION

Synthesis of *o*-CbzBiz, *m*-CbzBiz, and *p*-CbzBiz. Scheme 1 shows the synthetic routes for *o*-CbzBiz, *m*-CbzBiz, and *p*-CbzBiz. All three compounds were obtained in good yields (68−84%) by using 2-(4-bromophenyl)-1-phenyl-1*H*-benz[*d*]imidazole to react with the corresponding carbazole-containing boronic acid intermediates via palladium-catalyzed Suzuki coupling reactions. These carbazole-containing boronic acid intermediates were synthesized according to the previous literature.[16] All target compounds were soluble in common organic solvents such as toluene, dichloromethane, and chloroform, so they were characterized by ^{1}H NMR spectroscopy, ^{13}C NMR spectroscopy, and high-resolution mass spectrometry. It is worth noting that these compounds can be readily obtained through three synthetic steps in good yields, which is advantageous to host materials, which usually require larger amounts in OLED device fabrication.

Photophysical Properties. The UV−vis absorption and photoluminescence (PL) spectra of *o*-CbzBiz, *m*-CbzBiz, and *p*-CbzBiz are shown in Figure 1. The photophysical detail data are summarized in Table 1. There are two main absorption peaks (λ_{abs}) of these molecules. The peak located around 294 nm can be attributed to the localized $\pi-\pi^*$ transitions of carbazole and benzimidazole moieties, while the peak located around 310 to 327 nm can be attributed to the delocalized $\pi-\pi^*$ transitions of the whole molecule. By using the absorption onset values, the energy gaps of *o*-CbzBiz, *m*-CbzBiz, and *p*-CbzBiz were estimated to be 3.56, 3.54, and

https://dx.doi.org/10.1021/acsomega.0c00967
ACS Omega 2020, 5, 10553−10561

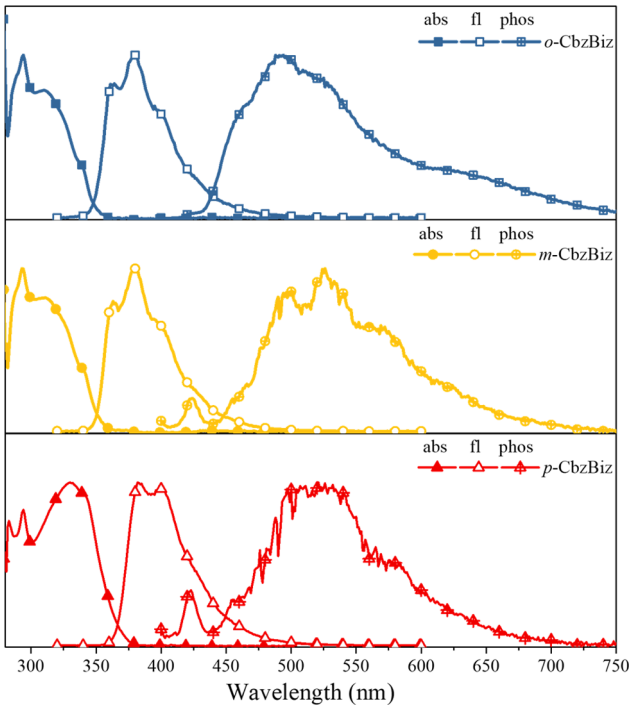

Figure 1. UV−vis absorption, fluorescence, and phosphorescence spectra of *o*-CbzBiz, *m*-CbzBiz, and *p*-CbzBiz in toluene.

3.37 eV. This result suggests that the effective conjugation length between the carbazole and the benzimidazole moieties of these molecules follows the order of *p*-CbzBiz > *m*-CbzBiz > *o*-CbzBiz. On the other hand, the main fluorescence emission peaks (λ_{em}) of *o*-CbzBiz, *m*-CbzBiz, and *p*-CbzBiz are located in a similar region (380−400 nm), which can be attributed to the charge transfer characteristics of these molecules at their excited states. This weak charge transfer characteristic can be further identified by the solvatochromic effect exhibited by these molecules. That is, their emission maximum slightly shifted to a longer wavelength as the polarity of solvents increased, which follows the order of dichloromethane > THF > toluene (Figure S1). The photoluminescence quantum yields (PLQYs) of *o*-CbzBiz, *m*-CbzBiz, and *p*-CbzBiz are 36, 12, and 88%, respectively. Only *p*-CbzBiz exhibited strong fluorescence in the solution state. Moreover, the phosphorescence spectra of *o*-CbzBiz, *m*-CbzBiz, and *p*-CbzBiz were measured in toluene at 77 K. By taking the highest-energy vibronic transition of the phosphorescence spectra, the triplet energy gaps of *o*-CbzBiz, *m*-CbzBiz, and *p*-CbzBiz were estimated to be 2.66, 2.48, and 2.45 eV, respectively. Among them, the triplet energy gap of *o*-CbzBiz is larger than that of CBP, i.e., 2.58 eV.[27] The high triplet energy of these molecules can be attributed to the 9-carbazole moiety, which reduces the exchange energies of the molecules.[28] It also makes these molecules suitable for the host materials for OLEDs. On the other hand, the singlet−triplet energy gaps (ΔE_{ST}) of *o*-CbzBiz, *m*-CbzBiz, and *p*-CbzBiz range from 0.90 to 1.06 eV, which is not favorable for the TADF phenomenon, and therefore, these molecules may not be applied as TADF emitters in OLEDs.

Thermal Properties. The thermal properties of *o*-CbzBiz, *m*-CbzBiz, and *p*-CbzBiz were analyzed by thermogravimetric analysis (TGA) and differential scanning calorimetry (DSC), and the data are collected in Table 1. These molecules exhibited high thermal-decomposition temperature (T_d, corresponding to 5% weight loss) ranging from 371 to 393 °C, which can be rationalized by the high structural rigidity of carbazole and benzimidazole moieties. In addition, the glass transition temperatures (T_g) for *o*-CbzBiz and *p*-CbzBiz were observed at 167 and 115 °C, respectively. These values are much higher than that of CBP, i.e., 62 °C, and could be beneficial to the thermal stability and lifetime of OLED devices.

Electrochemical Properties. To investigate the energy levels of *o*-CbzBiz, *m*-CbzBiz, and *p*-CbzBiz, we measured their oxidation potentials by cyclic voltammetry (CV). These molecules exhibited one quasi-reversible redox wave at similar potential due to oxidation of carbazole (Figure S2). Combining the oxidative potentials with the energy gaps obtained by the onset values of absorption bands, the HOMO and LUMO energy levels of these molecules were calculated and are summarized in Table 1. The HOMO energy levels of these molecules are similar, i.e., −5.73 to −5.74 eV, which suggests the weak electronic interaction between the carbazole and benzimidazole moieties within the molecule. On the other hand, the LUMO energy levels of these molecules are in the order of *o*-CbzBiz (−2.17 eV), *m*-CbzBiz (−2.20 eV) > *p*-CbzBiz (−2.36 eV), indicating that the molecular orbitals of benzimidazole are better stabilized by the neighboring biphenyl π-linker when carbazole is linked to its *para*-position rather than to its *meta*- and *ortho*-positions. Furthermore, the electrochemical stability of *o*-CbzBiz, *m*-CbzBiz, and *p*-CbzBiz was examined by measuring their cyclic voltammograms for four repeated cycles. The results in Figure S3 revealed that the redox curves were almost identical in four repeated cycles, indicating electrochemical stability of the host materials.

Theoretical Calculation. Density functional theory (DFT) on the spatial distribution of molecular orbitals and molecular geometry on *o*-CbzBiz, *m*-CbzBiz, and *p*-CbzBiz was performed to obtain the insight of their photophysical and electrochemical properties (Figure 2). In terms of their distribution of molecular orbitals (MOs), the HOMOs of *o*-CbzBiz and *m*-CbzBiz are mainly located on the carbazole and its adjacent phenyl unit, while the HOMO of *p*-CbzBiz is located not only on the carbazole and its adjacent phenyl unit but also extended to the benzimidazole moiety. On the other hand, all the LUMOs of *o*-CbzBiz, *m*-CbzBiz, and *p*-CbzBiz are

Table 1. Optical Properties and Electrochemical Properties for *o*-CbzBiz, *m*-CbzBiz, and *p*-CbzBiz

host	$T_m/T_g/T_d$ [°C]	λ_{abs}[a] [nm]	λ_{em}[a] [nm]	λ_{phos}[b] [nm]	PLQY [%]	HOMO/LUMO[c] [eV]	E_g[d] [eV]	E_T[e] [eV]
o-CbzBiz	273/167/371	294, 310	380	491	36	−5.73/−2.17	3.56	2.66
m-CbzBiz	326/na/377	293, 312	380	526	12	−5.74/−2.20	3.54	2.48
p-CbzBiz	296/115/393	294, 327	400	526	88	−5.73/−2.36	3.37	2.45

[a]Measured in toluene at room temperature. [b]Measured in toluene at 77 K. [c]Determined by cyclic voltammetry and the onset of the absorption band. [d]The optical band gap, determined by the onset of the absorption band. [e]Calculated by the highest-energy vibronic transition of the phosphorescence spectra measured at 77 K.

https://dx.doi.org/10.1021/acsomega.0c00967
ACS Omega 2020, 5, 10553−10561

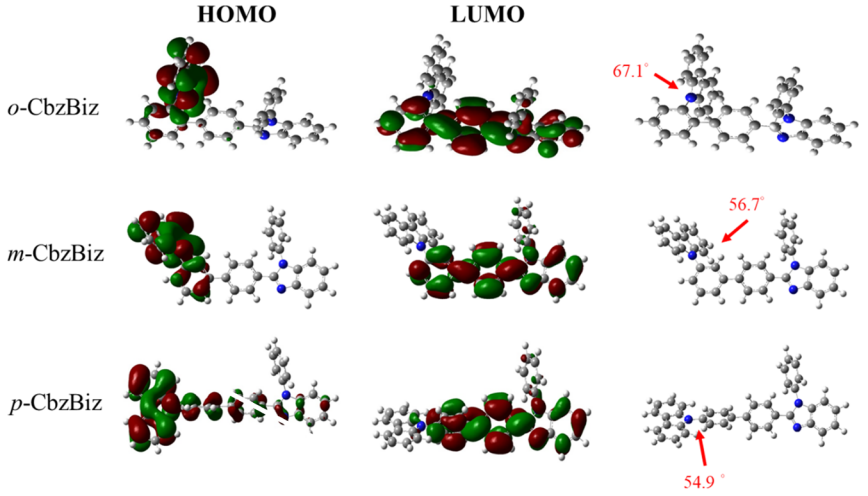

Figure 2. Molecular orbital distributions and molecular geometries of *o*-CbzBiz, *m*-CbzBiz, and *p*-CbzBiz.

mainly located on the benzimidazole and its adjacent biphenyl unit. The separated HOMOs and LUMOs ensure the bipolar characteristics of these molecules. In addition, the HOMO and LUMO distributions of *p*-CbzBiz are more overlapped than those of *o*-CbzBiz and *m*-CbzBiz. It can be explained by the smaller dihedral angle (54.9°) between the plane of carbazole and the plane of its phenyl unit of *p*-CbzBiz than those of *o*-CbzBiz (67.1°) and *m*-CbzBiz (56.7°). It also explains why *p*-CbzBiz exhibited the most effective conjugation length among these molecules. Moreover, the large dihedral angles suggest the twisted structures of these molecules, which explains the weak electronic interaction between the carbazole and benzimidazole moieties found via their electrochemical properties.

Device Performance. In order to study the electroluminescence properties of the OLEDs by using *o*-CbzBiz, *m*-CbzBiz, and *p*-CbzBiz as host materials, we prepared three green phosphorescence OLEDs by employing a uniform device structure of ITO/HAT-CN (15 nm)/TAPC (30 nm)/Ir(ppy)$_2$(acac) in hosts (10 wt %; 30 nm)/B3PyMPM (50 nm)/LiF (1 nm)/Al (100 nm) (device P, representing a phosphorescent emitter), and the energy level diagrams of the materials used in these devices are plotted in Figure 3a. In these devices, HAT-CN was used as the hole-injection layer (HIL), TAPC was used as the hole-transporting layer (HTL), Ir(ppy)$_2$(acac) was used as the phosphorescence emitter, B3PyMPM was used as an electron-transporting layer (ETL), and LiF was used as an electron-injection layer (EIL). A reference device applying CBP as the host material is also fabricated. Figure 4 shows the electroluminescence performances of these devices, while their characteristic data are summarized in Table 2. The maximum external quantum efficiencies (η_{ext}) for devices P1, P2, and P3 were 8.3 (η_c = 31.4 cd A^{-1} and η_p = 12.3 cd m^{-2}), 19.3 (η_c = 73.5 cd A^{-1} and η_p = 59.8 cd m^{-2}), and 21.8% (η_c = 83.3 cd A^{-1} and η_p = 74.8 cd m^{-2}), respectively. Device P3 showed the best performance among these devices. This phenomenon can be explained by the proper alignment of energy levels when *p*-CbzBiz was applied in the device using TAPC as HTL and B3PyMPM as ETL. It could also be attributed to the high PLQY of the 10% Ir(ppy)$_2$(acac)-doped *p*-CbzBiz film, i.e., 57.6%. The maximum η_{ext} for device P3 (21.8%) was comparable with that of the CBP-hosted device (22.1%). In addition, we also noted that device P3 exhibited lower efficiency roll-off than the CBP-hosted device (Figure 4c), suggesting that charge transporting was more balanced when *p*-CbzBiz was applied as the host. Furthermore, Figure S4 shows that the hole-transporting and electron-transporting mobility values of *p*-CbzBiz were 5.69 × 10^{-8} and 5.27 × 10^{-7} cm^2 V^{-1}·s^{-1}, respectively, which further demonstrated the bipolar property of *p*-CbzBiz. In addition, the stability of *p*-CbzBiz as a host material was studied by examining the lifetime of the device. With an initial luminance of 1000 nits, we found that the luminance of the CBP-hosted device decayed more than 85% after 10 h, while that of device P3 decayed only 10% under the same conditions (Figure S5). Apparently, *p*-CbzBiz exhibited better stability than CBP as a host material in OLED devices.

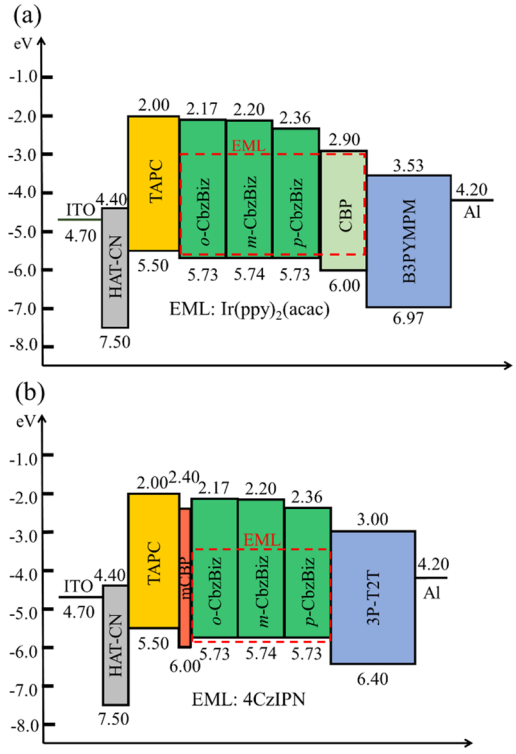

Figure 3. (a) Energy level diagram of green PhOLEDs; (b) energy level diagram of green TADF OLEDs.

https://dx.doi.org/10.1021/acsomega.0c00967
ACS Omega 2020, 5, 10553−10561

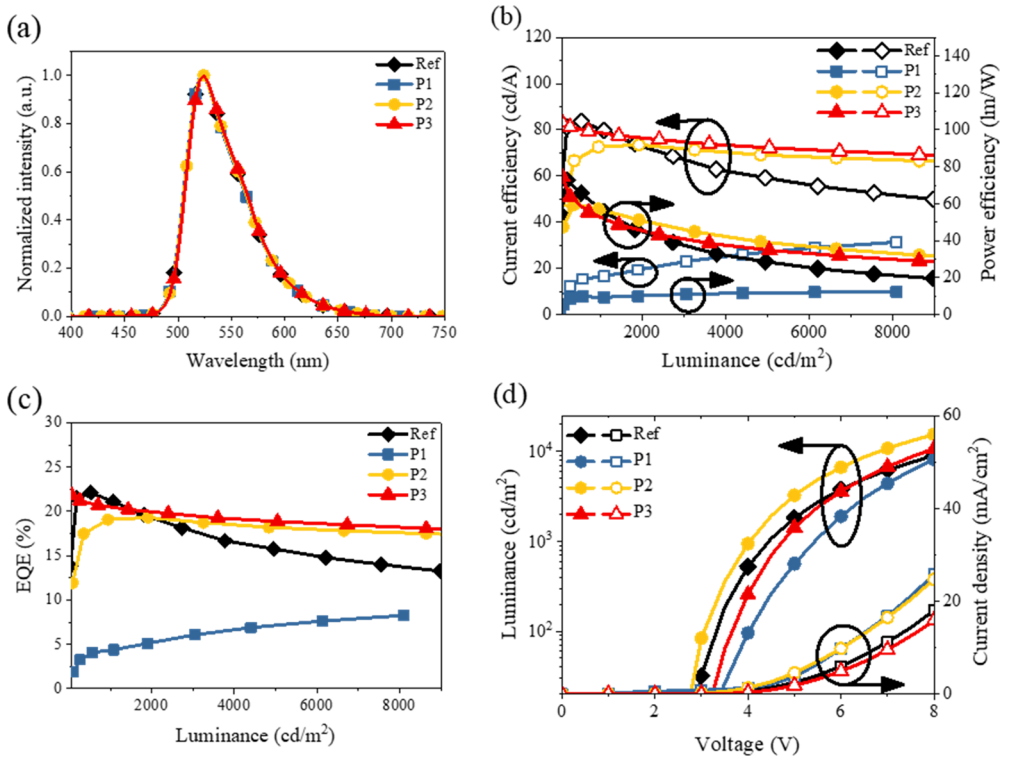

Figure 4. (a) Electroluminescence spectra; (b) current and power efficiency; (c) external quantum efficiency (EQE) versus luminance and (d) the current density−voltage−luminance (J−V−L), for PhOLEDs.

Table 2. Electroluminescence Characteristics of Green OLEDs with *o*-CbzBiz, *m*-CbzBiz, and *p*-CbzBiz

					η_{ext} [%]			
device	host	V_{on}	η_c [cd A^{-1}] max., 100, 1000 cd m^{-2}	η_p [lm W^{-1}] max., 100, 1000 cd m^{-2}	maximum	@100 cd m^{-2}	@1000 cd m^{-2}	CIE @max
P1	*o*-CbzBiz	3.0	31.4, 7.2, 16.6	12.3, 5.6, 9.5	8.3	1.9	4.4	(0.30, 0.65)
P2	*m*-CbzBiz	2.0	73.5, 72.6, 65.4	59.8, 57.0, 29.4	19.3	19.1	17.3	(0.30, 0.65)
P3	*p*-CbzBiz	2.5	83.3, 83.3, 79.4	74.8, 74.8, 55.5	21.8	20.7	21.8	(0.30, 0.65)
ref	CBP	2.5	79.7, 51.9, 79.7	55.6, 55.1, 55.6	22.1	13.8	21.5	(0.28, 0.65)
F1	*o*-CbzBiz	2.5	52.9, 52.9, 45.7	41.6, 41.6, 28.7	16.7	16.7	13.9	(0.30, 0.59)
F2	*m*-CbzBiz	3.0	41.7, 39.9, 41.6	27.9, 27.9, 21.7	13.2	12.9	12.8	(0.35, 0.57)
F3	*p*-CbzBiz	2.0	22.9, 22.9, 20.7	18.0, 18.0, 11.8	6.7	6.7	6.0	(0.32, 0.59)

On the other hand, the TADF OLEDs using devices 4CzIPN as emitters (devices F, representing delayed fluorescence emitters) were also fabricated using the device structure of ITO/HAT-CN (15 nm)/TAPC (30 nm)/mCBP (5 nm)/4CzIPN in hosts (9 wt %; 25 nm)/3P-T2T (50 nm)/LiF (1 nm)/Al (100 nm). The electroluminescence performances of these devices are shown in Figure 5 and Table 2. The energy level diagrams of the materials used in these devices are plotted in Figure 3b. As shown in Figure 5a, the emission peaks of the three devices are located from 520 to 536 nm, representing the effective energy transfer from the host to the TADF emitters, i.e., 4CzIPN. The η_{ext} values for devices F1, F2, and F3 were 16.7 (η_c = 52.9 cd A^{-1} and η_p = 41.6 cd m^{-2}), 13.2 (η_c = 41.7 cd A^{-1} and η_p = 26.1 cd m^{-2}), and 6.7% (η_c = 22.9 cd A^{-1} and η_p = 18.0 cd m^{-2}), respectively. The triplet energy of 4CzIPN was reported to be 2.40 eV in a previous study.[29] Therefore, the highest η_{ext} of device F1 among these devices can be attributed to the highest triplet energy of *o*-CbzBiz among the hosts, i.e., 2.66 eV, which ensures the effective energy transfer from *o*-CbzBiz to 4CzIPN. In addition, the PLQY of the 9% 4CzIPN-doped *o*-CbzBiz film was 93.9%, which also explains the high performance of the *o*-CbzBiz-hosted device. The performance of device F1 is either slightly higher than or comparable to that of other devices using carbazole-based hosts reported in the previous literature,[16,30−33] suggesting that the carbazole/benzimidazole-based hosts developed in this work are also promising hosts for TADF emitters.

CONCLUSIONS

We synthesized three bipolar molecules, i.e., *o*-CbzBiz, *m*-CbzBiz, and *p*-CbzBiz, by using carbazole as the electron donor, biphenyl as the π-bridge, and benzimidazole as the electron acceptor. Compared to a well-known carbazole-based host material CBP, it was found that the thermal stability of the molecules was significantly enhanced by introducing the benzimidazole moiety to carbazole-based molecules. Theoretical calculations on the geometries of these molecules show that the dihedral angle between the carbazole donor and the biphenyl π-bridge is large, resulting in the weak electronic coupling between the carbazole and benzimidazole moieties within the molecules, and therefore, high triplet energies of

https://dx.doi.org/10.1021/acsomega.0c00967
ACS Omega 2020, 5, 10553−10561

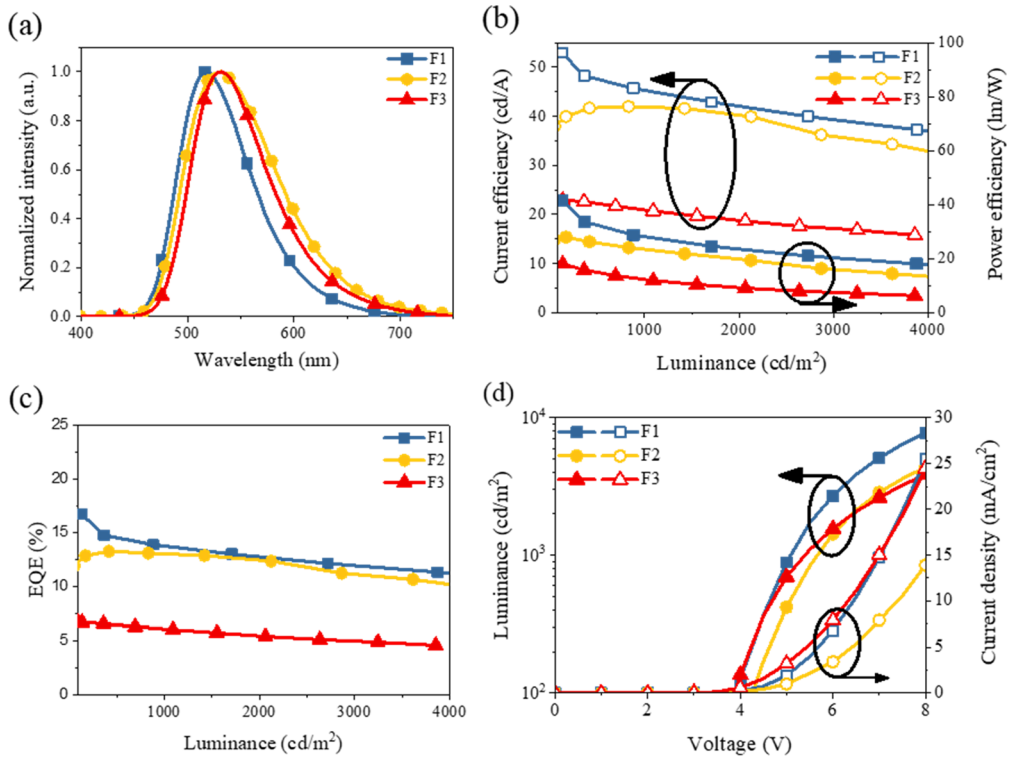

Figure 5. (a) Electroluminescence spectra; (b) current and power efficiency; (c) external quantum efficiency (EQE) versus luminance and (d) the current density−voltage−luminance (J−V−L), for TADF OLEDs.

these molecules were observed. This feature makes them suitable for the host materials in OLED devices. In terms of their electroluminescence properties, the highest performance of phosphorescent OLEDs with the *p*-CbzBiz as the host for $Ir(ppy)_2(acac)$ (η_{ext} = 21.8%, η_c = 83.3 cd A^{-1}, and η_p = 74.8 cd m^{-2}) was achieved, while the highest performance of TADF OLEDs was achieved when the *o*-CbzBiz was used as the host for 4CzIPN (η_{ext} = 16.7%, η_c = 52.9 cd A^{-1}, and η_p = 41.6 cd m^{-2}). These devices exhibited lower efficiency roll-off and comparable performance comparable to the CBP-hosted devices using the same emitters, suggesting that carbazole/benzimidazole-based bipolar molecules could be ideal hosts in the OLEDs with high efficiency for both phosphorescence and TADF emitters.

EXPERIMENTAL SECTION

Materials and Methods. All chemicals were purchased from Acros, Sigma-Aldrich, and TCI and were not purified before use. Toluene and THF were dried over by a solvent purification system. All reactions were performed under a nitrogen atmosphere and tracked by thin-layer chromatography. Products were purified by silica gel column chromatography (70−230 mesh, SiliCycle Inc.). ^1H and ^{13}C NMR spectra were measured on a Bruker (AC 300/AV 600 MHz) spectrometer in $CDCl_3$. Absorption spectra were measured on a Thermo Scientific Evolution 60s UV−vis spectrophotometer. For the intrinsic property characterizations, i.e., emission, transient photoluminescence (TRPL), and PL quantum yield (QY), the samples were put in a homemade holder with a spectrometer (Horiba FluoroMax Plus) in a nitrogen-filled environment to avoid any chemical reaction. In the PL and PLQY measurements, the sample was recorded with a 305 nm xenon lamp as an excitation light source (power density: 8.7 × 10^{-5} W m^{-2}). For film PLQY, an organic thin film (~80 nm) was applied on the quartz substrate by using thermal evaporation. For the TRPL, the light source of nanosecond pulsed excitation (Horiba N-320; power density: 3.3 × 10^{-5} W m^{-2}) was used for the transient measurement. The differential scanning calorimetry (DSC) measurements were performed on a PerkinElmer Pyris 1 DSC unit at a heating rate of 10 °C min^{-1} under nitrogen. Thermogravimetric analysis (TGA) was performed on a PerkinElmer Pyris 1 TGA instrument at a heating rate of 10 °C min^{-1} under nitrogen. Melting point measurements were carried out on an SRS OptiMelt MPA 100, and applied software was used to control the heating rate and determine the melting point. All redox measurements were executed in dichloromethane containing a 1 mM sample and 0.1 M supporting electrolyte [tetrabutylammonium hexafluorophosphate ($TBAPF_6$)] and purged for 10 min with N_2. The three-electrode system contained a glassy-carbon working electrode, a platinum counter electrode, and an Ag/AgCl reference electrode. The redox coupling of ferrocene/ferrocenium (Fc/Fc^+) was used as an external standard, and the scan rate was 100 mV s^{-1}. The oxidation potentials (E_{ox}) were estimated averaging maximal anodic and cathodic peak potentials. Fc/Fc^+ was converted to NHE by addition of 0.48 V. Energy gaps were calculated from the onset of the absorption band in toluene.

Device Fabrication and Characterization. In the device fabrication, the materials of 1,4,5,8,9,11-hexaazatriphenylenehexacarbonitrile (HAT-CN), 4,4′-cyclohexylidenebis[*N*,*N*-bis(4-methylphenyl)benzenamine] (TAPC), 3,3′-di(9*H*-carbazol-9-yl)-1,1′-biphenyl (mCBP), bis[2-(2-pyridinyl-*N*)phenyl-*C*](acetylacetonato)iridium(III) ($Ir(ppy)_2(acac)$), 2,4,5,6-tetra(9*H*-carbazol-9-yl)isophthalonitrile (4CzIPN), 2,4,6-tris(3-(1*H*-pyrazol-1-yl)phenyl)-1,3,5-triazine (3P-T2T), lithium flu-

https://dx.doi.org/10.1021/acsomega.0c00967
ACS Omega 2020, 5, 10553−10561

oride (LiF), and aluminum (Al) were purchased from Shine Materials Technology Co., Ltd. Afterward, all organic materials were sublimated twice using a homemade vacuum purification system (~8 × 10^{-6} torr). For the fabrication of OLEDs, the ITO substrates were cleaned with acetone and isopropyl alcohol in an ultrasonic bath and blowing nitrogen gas in ambient conditions. Then the ITO samples were transferred to a thermal evaporation system with a vacuum level of ~5 × 10^{-6} torr to deposit the organic and metal layers. For the deposition process of the organic layer, all thin films were fixed at a constant rate of 1 Å s^{-1} where the total thickness was monitored by quartz crystal measurement. On the other hand, for the device characterization, the OLED's brightness−current density−voltage characteristics, emission spectrum, and external quantum efficiency were measured by a customized setup of an integrating sphere, which consisted of a connection of a spectrometer (Ocean Optics USB2000) and a source meter (Keithley 2400). The software Labview controlled all programs and data acquisitions.

Measurement of Charge Mobility of the Materials. To calculate the charge mobility of organic materials, we prepared the hole-only [ITO/MoO_3 (20 nm)/*p*-CbzBiz (100 nm)/MoO_3 (20 nm)/Al (120 nm)]- and electron-only [Al (120 nm)/Cs_2CO_3 (1 nm)/*p*-CbzBiz (100 nm)/Cs_2CO_3 (1 nm)/Al (120 nm)]-based devices for measuring the space charge limiting current. Then the electrical characteristics can be fitted by the well-known Mott−Gurney equation, as shown below. However, such a method was followed by previous work to determine the charge mobility of organic materials with a thin thickness less than 120 nm[34]

$$J = \frac{9}{8}\varepsilon\varepsilon_0\mu\frac{V^2}{d^3} \quad (1)$$

where J is the hole- or electron-only device's current density, ε is the relative permittivity of the active material, ε_0 is the permittivity of vacuum, V is the applied voltage, and d is the thickness of the organic thin film.

Theoretical Calculation. All calculations were carried out in this study with the Gaussian 09 software. For these compounds, the geometric optimization calculations were performed by using the DFT-B3LYP method with the 6-31G* method.

Synthetic Procedure and Characterization for *o*-CbzBiz, *m*-CbzBiz, and *p*-CbzBiz. Compounds *o*-CbzBiz, *m*-CbzBiz, and *p*-CbzBiz were synthesized by similar procedures. 9-(2-Bromophenyl)-9*H*-carbazole, 9-(3-bromophenyl)-9*H*-carbazole, and 9-(4-bromophenyl)-9*H*-carbazole were synthesized according to previous procedures. Only the preparation of *o*-CbzBiz will be described in detail.

Synthesis of 9-(4′-(1-Phenyl-1H-benzo[d]imidazol-2-yl)-[1,1′-biphenyl]-2-yl)-9H-carbazole (o-CbzBiz). In a nitrogen atmosphere, a mixture of 9-(2-bromophenyl)-9*H*-carbazole (0.500 g, 1.551 mmol) was dissolved in dry THF (5 mL) and cooled to −78 °C, and then *n*-BuLi (1.900 mL, 3.040 mmol, 1.6 M in hexanes) was added dropwise. After the addition, the solution was brought up to 0 °C, stirred for 30 min, and then cooled to −78 °C again. Triisopropyl borate (0.437 mg, 2.327 mmol) was added slowly, and then the reaction solution was brought back to room temperature and stirred overnight. The reaction solution was added with 1 M HCl solution and stirred for 1 h, and then the reaction was quenched by pouring the whole solution into distilled water and then extracted with ethyl acetate. The organic layer was dried over anhydrous $MgSO_4$ and removed under reduced pressure. The crude product was mixed with $Pd(PPh_3)_4$ (90 mg, 0.140 mmol), 2-(4-bromophenyl)-1-phenyl-1*H*-benzo[*d*]imidazole (487 mg, 1.397 mmol), and 2 M K_2CO_3 solution (4 mL) that was dissolved in toluene/THF (2:1) and heated to reflux for 48 h. After that, the reaction was cooled down to room temperature, quenched with distilled water, and extracted with ethyl acetate. The organic layer was dried over anhydrous $MgSO_4$ and removed under reduced pressure. The crude product was purified by column chromatography using ethyl acetate/hexanes (1:5 by volume) as the eluent to give *o*-CbzBiz as a pale yellow solid (601 mg, 84.2% yield). ^{1}H NMR (600 MHz, $CDCl_3$): δ (ppm) = 8.04 (d, J = 7.8 Hz, 2H), 7.79 (d, J = 7.8 Hz, 1H), 7.67 (d, J = 7.8 Hz, 1H), 7.60−7.55 (m, 2H), 7.51 (d, J = 7.8 Hz, 1H), 7.40−7.36 (m, 3H), 7.29−7.25 (m, 3H), 7.22−7.16 (m, 6H), 7.04−7.02 (m, 4H), 6.96 (d, J = 7.8 Hz, 2H). ^{13}C NMR (75 MHz, $CDCl_3$): δ (ppm) = 151.83, 142.97, 140.96, 139.78, 137.00, 136.70, 134.87, 131.38, 129.79, 129.72, 129.27, 129.13, 128.79, 128.66, 128.20, 127.66, 127.07, 125.67, 123.24, 123.12, 122.91, 120.09, 119.75, 119.55, 110.32, 109.86. m/z: $[M]^+$ calcd for $C_{37}H_{25}N_3$, 511.2048; found, 511.2049.

Synthesis of 9-(4′-(1-Phenyl-1H-benzo[d]imidazol-2-yl)-[1,1′-biphenyl]-3-yl)-9H-carbazole (m-CbzBiz). A pale yellow solid (551 mg, 77.1% yield). ^{1}H NMR (600 MHz, $CDCl_3$): δ (ppm) = 8.16 (d, J = 7.8 Hz, 2H), 7.91 (d, J = 7.8 Hz, 1H), 7.78 (s, 1H), 7.71−7.66 (m, 4H), 7.60 (d, J = 7.8 Hz, 2H), 7.57−7.52 (m, 3H), 7.49 (d, J = 7.2 Hz, 2H), 7.45−7.41 (m, 4H), 7.37−7.35 (m, 3H), 7.31−7.25 (m, 4H). ^{13}C NMR (75 MHz, $CDCl_3$): δ (ppm) = 151.85, 143.08, 142.10, 140.92, 138.36, 137.39, 137.05, 130.37, 129.98, 129.46, 128.71, 127.50, 126.96, 126.39, 126.09, 126.00, 125.73, 123.44, 123.08, 120.36, 120.01, 119.90, 110.46, 109.73. m/z: $[M]^+$ calcd for $C_{37}H_{25}N_3$, 511.2048; found, 511.2040.

Synthesis of 9-(4′-(1-Phenyl-1H-benzo[d]imidazol-2-yl)-[1,1′-biphenyl]-4-yl)-9H-carbazole (p-CbzBiz). A pale yellow solid (973 mg, 67.9% yield). ^{1}H NMR (600 MHz, $CDCl_3$): δ (ppm) = 8.16 (d, J = 7.8 Hz, 2H), 7.93 (d, J = 7.8 Hz, 1H), 7.82 (d, J = 8.4 Hz, 2H), 7.72 (d, J = 8.4 Hz, 2H), 7.66−7.64 (m, 4H), 7.58−7.51 (m, 3H), 7.46−7.36 (m, 7H), 7.31−7.27 (m, 4H). ^{13}C NMR (75 MHz, $CDCl_3$): δ (ppm) =151.81, 142.94, 140.94, 140.14, 139.76, 136.98, 136.68, 134.85, 131.36, 129.77, 129.70, 129.25, 129.12, 128.78, 128.63, 128.18, 127.64, 127.05, 125.65, 123.22, 123.10, 122.90, 120.07, 119.73, 119.53, 110.30, 109.84. m/z: $[M]^+$ calcd for $C_{37}H_{25}N_3$, 511.2048; found, 511.2050.

■ ASSOCIATED CONTENT

Supporting Information

The Supporting Information is available free of charge at https://pubs.acs.org/doi/10.1021/acsomega.0c00967.

Detail information including solvatochromic study on emission spectra, cyclic voltammograms, TGA thermograms, ^{1}H, ^{13}C NMR, and high-resolution mass spectra of the host materials (PDF)

■ AUTHOR INFORMATION

Corresponding Authors

Bo-Cheng Wang − *Department of Chemistry, Tamkang University, New Taipei City 251, Taiwan*; Email: bcw@mail.tku.edu.tw

https://dx.doi.org/10.1021/acsomega.0c00967
ACS Omega 2020, 5, 10553−10561

Shun-Wei Liu − *Department of Electronic Engineering and Organic Electronics Research Center, Ming Chi University of Technology, New Taipei City 24301, Taiwan;* orcid.org/0000-0002-3128-905X; Email: swliu@mail.mcut.edu.tw

Chih-Hsin Chen − *Department of Chemistry, Tamkang University, New Taipei City 251, Taiwan;* orcid.org/0000-0001-5321-9696; Email: chc@mail.tku.edu.tw

Authors

Zhen-Jie Gao − *Department of Chemistry, Tamkang University, New Taipei City 251, Taiwan*

Tzu-Hung Yeh − *Department of Electronic Engineering and Organic Electronics Research Center, Ming Chi University of Technology, New Taipei City 24301, Taiwan; Department of Electronic Engineering, National Taiwan University of Science and Technology, Taipei 10607, Taiwan*

Jing-Jie Xu − *Department of Chemistry, Tamkang University, New Taipei City 251, Taiwan*

Chih-Chien Lee − *Department of Electronic Engineering, National Taiwan University of Science and Technology, Taipei 10607, Taiwan*

Anuradha Chowdhury − *Department of Electronic Engineering and Organic Electronics Research Center, Ming Chi University of Technology, New Taipei City 24301, Taiwan*

Complete contact information is available at: https://pubs.acs.org/10.1021/acsomega.0c00967

Notes

The authors declare no competing financial interest.

■ ACKNOWLEDGMENTS

We thank the Ministry of Science and Technology, Taiwan (MOST 107-2113-M-032-003, 108-2113-M-032-004, 108-2221-E-131-027-MY2, and 108-2221-E-011-151) and Department of Chemistry, Tamkang University for funding support. We also thank Prof. Ken-Tsung Wong from the Department of Chemistry, National Taiwan University for providing the electron-transporting materials, i.e., 3P-T2T, in this work.

■ REFERENCES

(1) Tang, C. W.; VanSlyke, S. A. Organic electroluminescent diodes. *Appl. Phys. Lett.* **1987**, *51*, 913−915.

(2) Huang, J.; Su, J.-H.; Li, X.; Lam, M.-K.; Fung, K.-M.; Fan, H.-H.; Cheah, K.-W.; Chen, C. H.; Tian, H. Bipolar anthracene derivatives containing hole- and electron-transporting moieties for highly efficient blue electroluminescence devices. *J. Mater. Chem.* **2011**, *21*, 2957−2964.

(3) Sasabe, H.; Kido, J. Development of high performance OLEDs for general lighting. *J. Mater. Chem. C* **2013**, *1*, 1699−1707.

(4) Kelley, T. W.; Baude, P. F.; Gerlach, C.; Ender, D. E.; Muyres, D.; Haase, M. A.; Vogel, D. E.; Theiss, S. D. Recent progress in organic electronics: Materials, devices, and processes. *Chem. Mater.* **2004**, *16*, 4413−4422.

(5) Yang, Z.; Mao, Z.; Xie, Z.; Zhang, Y.; Liu, S.; Zhao, J.; Xu, J.; Chi, Z.; Aldred, M. P. Recent advances in organic thermally activated delayed fluorescence materials. *Chem. Soc. Rev.* **2017**, *46*, 915−1016.

(6) Uoyama, H.; Goushi, K.; Shizu, K.; Nomura, H.; Adachi, C. Highly efficient organic light-emitting diodes from delayed fluorescence. *Nature* **2012**, *492*, 234−238.

(7) Yang, X.; Zhou, G.; Wong, W.-Y. Functionalization of phosphorescent emitters and their host materials by main-group elements for phosphorescent organic light-emitting devices. *Chem. Soc. Rev.* **2015**, *44*, 8484−8575.

(8) Park, J.-H.; Kim, E.-K.; El-Deeb, I. M.; Jung, S.-J.; Choi, D.-H.; Kim, D.-H.; Yoo, K.-H.; Kwon, J.-H.; Lee, S.-H. New bipolar green host materials containing benzimidazole-carbazole moiety in phosphorescent OLEDs. *Bull. Korean Chem. Soc.* **2011**, *32*, 841−846.

(9) Wu, C.; Wang, B.; Wang, Y.; Hu, J.; Jiang, J.; Ma, D.; Wang, Q. A universal host material with a simple structure for monochrome and white phosphorescent/TADF OLEDs. *J. Mater. Chem. C* **2019**, *7*, 558−566.

(10) Cui, L.-S.; Xie, Y.-M.; Wang, Y.-K.; Zhong, C.; Deng, Y.-L.; Liu, X.-Y.; Jiang, Z.-Q.; Liao, L.-S. Pure hydrocarbon hosts for≈100% exciton harvesting in both phosphorescent and fluorescent light-emitting devices. *Adv. Mater.* **2015**, *27*, 4213−4217.

(11) Cho, Y. J.; Yook, K. S.; Lee, J. Y. A universal host material for high external quantum efficiency close to 25% and long lifetime in green fluorescent and phosphorescent OLEDs. *Adv. Mater.* **2014**, *26*, 4050−4055.

(12) Baldo, M. A.; Lamansky, S.; Burrows, P. E.; Thompson, M. E.; Forrest, S. R. Very high-efficiency green organic light-emitting devices based on electrophosphorescence. *Appl. Phys. Lett.* **1999**, *75*, 4−6.

(13) Jhulki, S.; Moorthy, J. N. Small molecular hole-transporting materials (HTMs) in organic light-emitting diodes (OLEDs): structural diversity and classification. *J. Mater. Chem. C* **2018**, *6*, 8280−8325.

(14) Chatterjee, T.; Wong, K.-T. Perspective on host materials for thermally activated delayed fluorescence organic light emitting diodes. *Adv. Opt. Mater.* **2019**, *7*, 1800565.

(15) Holmes, R. J.; Forrest, S. R.; Tung, Y.-J.; Kwong, R. C.; Brown, J. J.; Garon, S.; Thompson, M. E. Blue organic electrophosphorescence using exothermic host-guest energy transfer. *Appl. Phys. Lett.* **2003**, *82*, 2422−2424.

(16) Song, W.; Chen, Y.; Xu, Q.; Mu, H.; Cao, J.; Huang, J.; Su, J. [1, 2, 4] Triazolo [1, 5-a] pyridine-based host materials for green phosphorescent and delayed-fluorescence OLEDs with low efficiency roll-off. *ACS Appl. Mater. Interfaces* **2018**, *10*, 24689−24698.

(17) Tokito, S.; Iijima, T.; Suzuri, Y.; Kita, H.; Tsuzuki, T.; Sato, F. Confinement of triplet energy on phosphorescent molecules for highly-efficient organic blue-light-emitting devices. *Appl. Phys. Lett.* **2003**, *83*, 569−571.

(18) Lee, C. W.; Lee, J. Y. Highly electron deficient pyrido-[3′,2′:4,5]furo[2,3-b]pyridine as a core structure of a triplet host material for high efficiency green phosphorescent organic light-emitting diodes. *Chem. Commun.* **2013**, *49*, 6185−6187.

(19) Liu, B.; Zhao, J.; Luo, C.; Lu, F.; Tao, S.; Tong, Q. A novel bipolar phenanthroimidazole derivative host material for highly efficient green and orange-red phosphorescent OLEDs with low efficiency roll-off at high brightness. *J. Mater. Chem. C* **2016**, *4*, 2003−2010.

(20) Chen, Y.; Wei, X.; Cao, J.; Huang, J.; Gao, L.; Zhang, J.; Su, J.; Tian, H. Novel bipolar indole-based solution-processed host material for efficient green and red phosphorescent OLEDs. *ACS Appl. Mater. Interfaces* **2017**, *9*, 14112−14119.

(21) Wang, Y.; Song, W.; Chen, Y.; Jiang, Y.; Mu, H.; Huang, J.; Su, J. A series of new bipolar CBP derivatives with introduction of a electron-deficient moiety for efficient green organic light-emitting diodes. *Org. Electron.* **2018**, *61*, 142−150.

(22) Song, W.; Gao, L.; Zhang, T.; Huang, J.; Su, J. [1,2,4]Triazolo-[1,5-a]pyridine based host materials for high-performance red PhOLEDs with external quantum efficiencies over 23%. *J. Lumin.* **2019**, *206*, 386−392.

(23) Chang, S.-Y.; Lin, G.-T.; Cheng, Y.-C.; Huang, J.-J.; Chang, C.-L.; Lin, C.-F.; Lee, J.-H.; Chiu, T.-L.; Leung, M.-K. Construction of highly efficient carbazol-9-yl-substituted benzimidazole bipolar hosts for blue phosphorescent light-emitting diodes: Isomer and device performance relationships. *ACS Appl. Mater. Interfaces* **2018**, *10*, 42723−42732.

(24) Zhao, Y.; Wu, C.; Qiu, P.; Li, X.; Wang, Q.; Chen, J.; Ma, D. New benzimidazole-based bipolar hosts: highly efficient phosphorescent and thermally activated delayed fluorescent organic light-emitting diodes employing the same device structure. *ACS Appl. Mater. Interfaces* **2016**, *8*, 2635−2643.

(25) Shizu, K.; Uejima, M.; Nomura, H.; Sato, T.; Tanaka, K.; Kaji, H.; Adachi, C. Enhanced electroluminescence from a thermally activated delayed-fluorescence emitter by suppressing nonradiative decay. *Phys. Rev. Appl.* **2015**, *3*, No. 014001.
(26) Sato, K.; Shizu, K.; Yoshimura, K.; Kawada, A.; Miyazaki, H.; Adachi, C. Organic luminescent molecule with energetically equivalent singlet and triplet excited states for organic light-emitting diodes. *Phys. Rev. Lett.* **2013**, *110*, 247401.
(27) Schrögel, P.; Tomkevičienė, A.; Strohriegl, P.; Hoffmann, S. T.; Köhler, A.; Lennartz, C. A series of CBP-derivatives as host materials for blue phosphorescent organic light-emitting diodes. *J. Mater. Chem.* **2011**, *21*, 2266−2273.
(28) Bui, T.-T.; Goubard, F.; Ibrahim-Ouali, M.; Gigmes, D.; Dumur, F. Thermally activated delayed fluorescence emitters for deep blue organic light emitting diodes: A review of recent advances. *Appl. Sci.* **2018**, *8*, 494.
(29) Nakanotani, H.; Masui, K.; Nishide, J.; Shibata, T.; Adachi, C. Promising operational stability of high-efficiency organic light-emitting diodes based on thermally activated delayed fluorescence. *Sci. Rep.* **2013**, *3*, 2127.
(30) Li, J.; Dong, S.-C.; Opitz, A.; Liao, L.-S.; Koch, N. Design principles of carbazole/dibenzothiophene derivatives as host material in modern efficient organic light-emitting diodes. *J. Mater. Chem. C* **2017**, *5*, 6989−6996.
(31) Cai, M.; Song, X.; Zhang, D.; Qiao, J.; Duan, L. π-π stacking: a strategy to improve the electron mobilities of bipolar hosts for TADF and phosphorescent devices with low efficiency roll-off. *J. Mater. Chem. C* **2017**, *5*, 3372−3381.
(32) Li, S.-W.; Yu, C.-H.; Ko, C.-L.; Chatterjee, T.; Hung, W.-Y.; Wong, K.-T. Cyanopyrimidine-carbazole hybrid host materials for high-efficiency and low-efficiency roll-off TADF OLEDs. *ACS Appl. Mater. Interfaces* **2018**, *10*, 12930−12936.
(33) Li, W.; Li, J.; Wang, F.; Gao, Z.; Zhang, S. Universal host materials for high-efficiency phosphorescent and delayed-fluorescence OLEDs. *ACS Appl. Mater. Interfaces* **2015**, *7*, 26206−26216.
(34) Liu, S.-W.; Chang, Y.-T.; Lee, C.-C.; Yuan, C.-H.; Liu, L.-A.; Chen, Y.-S.; Lin, C.-F.; Wu, C.-I.; Chen, C.-T. Single-layer blue electrophosphorescent organic light-emitting diodes based on small-molecule mixed hosts: comparison between the solution and vacuum fabrication processes. *Jpn. J. Appl. Phys.* **2013**, *52*, No. 012101.

https://dx.doi.org/10.1021/acsomega.0c00967
ACS Omega 2020, 5, 10553−10561